Isodesmic Reactions for Transition States: Reactions of Cl Atoms with Methane and Halogenated Methanes

Vadim D. Knyazev

Research Center for Chemical Kinetics, Department of Chemistry, The Catholic University of America, Washington, D.C. 20064, and Physical and Chemical Properties Division, National Institute of Standards and Technology, Gaithersburg, Maryland 20899

Received: August 4, 2003; In Final Form: October 10, 2003

The performance of the technique of isodesmic reactions for transition states (IRTS) has been analyzed via application to 17 reactions of abstraction of hydrogen atoms from methane and halogenated methanes by Cl atom. A variety of quantum chemical methods and basis sets was used. The calculated energy barriers demonstrate linear correlations with those derived from modeling of the experimental rate constant data, in agreement with the prediction based on the IRTS formalism. The results of the study confirm the validity of the technique of isodesmic reactions for transition states for calculation of reaction rates and demonstrate the existence of method-specific systematic errors in calculations of reaction barriers. The technique of isodesmic reactions is directed at factoring out and eliminating these systematic errors. The predictive ability of the technique is directly related to the quality of the observed correlations. Average and maximum deviations from the best fit lines on the correlation plots depend on the quantum chemical method used. The highest quality correlation (the least amount of scatter, average deviation of 1.5 kJ mol^{-1} and maximum deviation of 3.5 kJ mol^{-1}) was obtained with the BH&HLYP/6-311+(3df,2pd)//BH&HLYP/6-311(d,p) combination of single-point energy//geometry optimization methods. Use of higher level methods such as spin-projected PMP4, QCISD(T), and CCSD(T) results in small systematic errors (1.4−5.9 kJ mol^{-1}) but larger scatter on the plots of the calculated barriers vs "experimental" barrier correlations (maximum deviations of 5.6−6.8 kJ mol^{-1}).

I. Introduction

Kinetic simulations are becoming more and more widely used in modeling of chemical processes of practical interest. Over the past two decades, the computer hardware and technology for solving systems of differential equations associated with large kinetic schemes have greatly improved. The main hindrance on the way toward progress is the limited knowledge of the rate constants of individual chemical reactions. While thorough experimental investigations remain the most reliable instrument for gathering such information, more and more chemists and engineers have come to the realization that it is, in general, unrealistic to attempt to obtain rate coefficients of all the important reactions in direct experiments. Instead, extensive sets of reliable experimental data should be used as benchmarks in order to identify computational tools capable of predicting the desired rate constants of cognate reactions of interest.

The need for computational tools capable of predicting rates of elementary chemical reactions with accuracy suitable for simulation of complex kinetic systems has resulted in a significant rise in the numbers of studies directed at developing such tools. Methods being developed range from those based on high-level quantum chemical studies of potential energy surfaces and rigorous theories of kinetics and dynamics to simpler and faster methods based on empirical correlations and analogies. An informative review of the current status of methods for a priori evaluation of rates of elementary chemical reactions can be found in ref 1.

Recently, a technique for computation of rate constants of elementary gas-phase reactions based on the use of the formalism of isodesmic reactions for transition states (IRTS) has been developed.[2] This technique has been demonstrated to yield the rates of abstraction of hydrogen and chlorine atoms from chloroalkanes by H atoms with a high degree of accuracy. Average deviations between calculated and experimental rate constant values were 17−24%, depending on the quantum chemical method used, although channel-specific rates showed larger divergence. The accuracy of the technique of isodesmic reactions for transition states, when applied to the reactions studied in ref 2, was significantly better than that of the more conventional method when quantum chemically generated barriers and properties of transition states are used directly to compute reaction rate constants.

In the current study, the performance of the technique of isodesmic reactions for transition states is analyzed via application to the reactions of abstraction of hydrogen atoms from methane and halogenated methanes by Cl atoms. The method of analysis applied here differs from that used in ref 2 in that linear correlations between the calculated energy barriers and those derived from modeling of the experimental rate constant data were examined. As demonstrated below, for reactions of atom abstraction, the basic postulate of the IRTS technique predicts the existence of such linear correlations. The results of the current study serve to validate the IRTS approach, although isodesmic reactions per se are not explicitly considered in the calculations involved.

The focus on the reactions of H with chloroalkanes (ref 2) and those of Cl with halomethanes (this work) was motivated, primarily, by the importance of the reactions of H and Cl atoms with chlorinated hydrocarbons (CHCs) in the reactive systems of combustion and incineration of CHCs. In CHC/O_2 and CHC/

10.1021/jp036281p CCC: $25.00
Published on Web 11/18/2003

hydrocarbon/O_2 flames, reactions of Cl and H atoms with CHCs together with unimolecular decomposition are the major channels of consumption of CHCs (e.g., refs 3−8; a more complete set of references can be found in ref 2). The results of numerical kinetic simulations demonstrate that the rates of CHC destruction and concentrations of active species are highly sensitive to the rates of H + CHC and Cl + CHC reactions. This study is a part of a project directed at elucidation of the kinetics of these important reactions; other parts of the project included experimental studies of the reactions of H and Cl atoms with chlorinated methanes and ethanes[9−12] and a computational study of the H + chloroalkanes reactions.[2]

Many of the reactions considered here have been studied theoretically before (e.g., refs 13−17). These studies are not discussed here as the current work is concerned, primarily, not with individual reactions but with systematic assessment of the accuracy and the predictive ability of a particular technique, that of isodesmic reactions for transition states.

This article is organized as follows. This section is an introduction. The computational methods used and results are described in sections II and III, respectively. A discussion is given in section IV.

II. Methods

II.1. Quantum Chemical Methods Used. In the quantum chemical calculations, three methods were used for the optimization of the geometrical structures of the involved species. The first two methods are MP2[18−20] and QCISD.[21] Both are rather demanding in terms of required computer resources when applied to molecules containing many chlorine atoms; calculations involving molecules with bromine atoms become even more problematic. Thus, a less computationally expensive BH&HLYP density functional method[22,23] (a version implemented in the Gaussian 98 program,[24,25] which, as described in the Gaussian manual, is different from that of ref 22) was also used. The choice of the BH&HLYP functional was based on the reported positive results of using this method for studies of the properties of transition states (see, for example, refs 26−31), including the results obtained in ref 2 using the approach of isodesmic reactions. The 6-311G(d,p) basis set was used in all the QCISD and most of the BH&HLYP structure optimization calculations; the 6-311G(2d,2p) basis set was used in most MP2 optimizations. Also, limited calculations were performed with correlation-consistent basis sets augmented with diffuse functions[32] (aug-cc-pvdz with MP2 and aug-cc-pvtz with BH&HLYP) to investigate basis set effects.

With each of the methods used for geometry optimization, a variety of higher level single-point energy calculations was used. With the UMP2/6-311G(2d,2p)-optimized geometries, one method is the spin-projected[33] PMP4(SDTQ)/6-311++G(3df,2p).[34] This PMP4(SDTQ)/6-311++G(3df,2p)//UMP2/6-311G(2d,2p) combination (including the UMP2/6-311G(2d,2p) vibrational frequencies) was recently demonstrated by Louis et al.[35−37] to result in good agreement with experimental data for a series of reactions of abstraction of a hydrogen atom from halogenated hydrocarbons by an OH radical. In the second approach, the QCISD(T)/6-311+G(2d,2p)[21] energy was used. In the study of the H + chloroalkanes reactions, both the PMP4-(SDTQ)/6-311++G(3df,2p) and the QCISD(T) methods with large basis sets produced good results when applied within the framework of the approach of isodesmic reactions for transition states.[2] The choice of other methods for single-point energy calculation was motivated by the desire to identify lower cost computational methods suitable for predictive calculations. These include the QCISD method, PMP2[33] with large basis sets (6-311++G(3df,2p) and 6-311++G(3df,2pd)), and density functional BH&HLYP and KMLYP[38,39] methods with the 6-311+G(3df,2p) basis set. Reference 40 can be consulted for the details of the methods and the basis sets used. The Gaussian 98 program[24,25] was used in all quantum chemical calculations.

II.2. The Technique of Isodesmic Reactions for Transition States (IRTS). Approach and Method of Analysis. *II.2.1. Isodesmic Reactions.* Isodesmic reactions, i.e., (usually) fictitious reactions that conserve the types of chemical bonds and their numbers, are often used in computational thermochemistry. The enthalpies of these reactions are usually obtained in quantum chemical calculations, and it is expected that computational errors that are specific to a particular bond type will, to a large extent, cancel on both sides of the chemical equation.

The technique of isodesmic reactions for transition states as applied to the reactions of H atoms with chloroalkanes in ref 2 consists of the following main elements. First, a reference reaction is selected for which highly accurate experimental data are available and thus the temperature dependence of the rate constant is well established. For this reaction, a transition state theory model is created on the basis of quantum chemical calculations. The model is adjusted to provide a match with the experimental data by varying two parameters: the barrier height $E_{0,\mathrm{REF}}$ and the preexponential correction factor F_A. Then transition state theory models of a series of cognate reactions are produced on the basis of same-level quantum chemical calculations. At this stage, these models include structures and vibrational frequencies of the species involved, reaction barrier widths,[11,12,42,43] but not barrier heights. In the next step, the energy barrier heights for these models are obtained from the value of $E_{0,\mathrm{REF}}$ and the 0 K enthalpies, $\Delta H_0^\circ{}_{\mathrm{ISO}}$, of isodesmic reactions of the type

$$\mathrm{TS} + \mathrm{reactants(REF)} = \mathrm{TS(REF)} + \mathrm{reactants} + \Delta H_0^\circ{}_{\mathrm{ISO}} \quad (1)$$

where TS, reactants, TS(REF), and reactants(REF) are the transition states and reactants of the particular reaction from the series and the reference reaction, respectively. Note that, computationally, transition states can be treated just like chemical species. Here, $\Delta H_0^\circ{}_{\mathrm{ISO}}$ values are obtained in quantum chemical calculations performed, generally, at a different (usually, higher) level of theory. The energy barriers for the reactions from the series are then calculated as

$$E_0 = E_{0,\mathrm{REF}} - \Delta H_0^\circ{}_{\mathrm{ISO}} \quad (\mathrm{I})$$

The rate constants of the reactions from the series are calculated using the thus created models and corrected via multiplying by the preexponential correction factor, F_A.

II.2.2. Method of Analysis. For the reactions of abstraction of H and Cl atoms by hydrogen atoms, isodesmic reactions of the types

$$\mathrm{H\cdots H\cdots R} + \mathrm{CH_4} = \mathrm{H\cdots H\cdots CH_3} + \mathrm{RH} \qquad (+\Delta H^\circ{}_0(2)) \quad (2)$$

$$\mathrm{H\cdots Cl\cdots R} + \mathrm{CCl_4} = \mathrm{H\cdots Cl\cdots CCl_3} + \mathrm{RCl} \qquad (+\Delta H^\circ{}_0(3)) \quad (3)$$

were used in ref 2 (here H···H···R and H···Cl···R are the corresponding transition states). Reactions of H atoms with methane and carbon tetrachloride represented clear cases of abstraction of H and Cl atoms, respectively, and thus provided

suitable choices for the reference reactions. Most of the other H + chloroalkane reactions included channels of both H and Cl abstraction. Since, for each of these reactions, existing experimental data provided only the temperature dependences of the rate constants for the overall reaction, comparison of theory with experiment could only be performed by examining the temperature dependences of these overall reaction rates.

In the current study, reactions of Cl atoms with halogenated methanes are considered. For all reactions of this class, the site of attack by Cl is unambiguous—it is that of the abstraction of an H atom. For any two reactions of this type

$$Cl + R_1H \rightarrow (Cl\cdots H\cdots R_1) \rightarrow HCl + R_1 \qquad (4)$$

$$Cl + R_2H \rightarrow (Cl\cdots H\cdots R_2) \rightarrow HCl + R_2 \qquad (5)$$

the following isodesmic reaction can be written:

$$Cl\cdots H\cdots R_1 + R_2H = Cl\cdots H\cdots R_2 + R_1H \qquad (+\Delta H^\circ_0(6)) \qquad (6)$$

(Here, $Cl\cdots H\cdots R_1$ and $Cl\cdots H\cdots R_2$ denote the transition states.) Thus, any reaction from the class for which the temperature dependence of the rate constant is well established can be used as a reference reaction. Also, comparison of the calculated and the experimental rate constants can be performed directly, without any complications due to different reaction channels.

The absence of ambiguity in the site of attack and the availability of experimental rate constant data on several different reactions present an opportunity for a different way of assessing the performance of the technique of isodesmic reactions for transition states. The enthalpy of the isodesmic reaction 6 is equal to the difference between the energy barriers of reactions 4 and 5, as can be seen by formally adding Cl to both sides of the chemical equation 6. Thus, the primary postulation of the technique of isodesmic reactions is equivalent to the assumption that, although a particular quantum chemical method may not yield accurate absolute values of energy barriers, differences between the energy barriers of individual reactions can be calculated with a high degree of accuracy for a series of reactions of the same type. Examination of the plots of computed vs "experimental" energy barriers for a series of reactions of the same type can provide an evaluation of the validity of this hypothesis. Such plots should form straight lines with slopes equal to unity and, generally, a nonzero *Y*-axis intercept. This intercept reflects a systematic error in the calculation of barriers specific to the quantum chemical method used. The performance of the technique of isodesmic reactions in combination with various quantum chemical methods was evaluated in the current study using this approach. Linear correlations of calculated vs "experimental" energy barriers were examined. Average and maximum deviations within sets of reactions served as quantitative measures of the accuracy of the technique/quantum chemical method combinations.

II.2.3. "Experimental" Energy Barriers and Preexponential Factors. Knowledge of energy barriers can be extracted from the experimental rate constant data only through modeling, e.g., by fitting model parameters to reproduce the experimental data. The results will be dependent on the details of the particular model and rate theory used. It can be expected, however, that, if the same kind of modeling is uniformly applied to the rates of a series of reactions of the same class, the resultant values of the "experimental" energy barriers obtained through the same prism of theory will have similar errors (compared with the real barrier values) for all reactions considered.

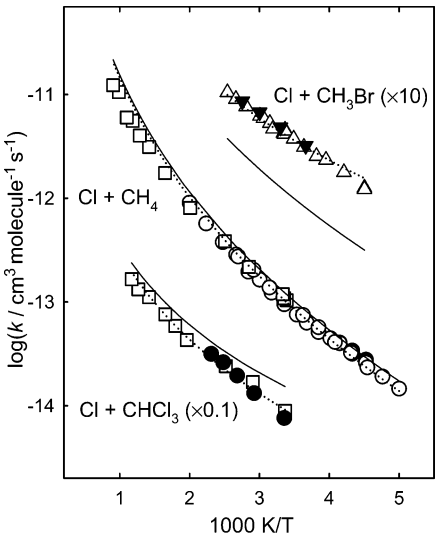

Figure 1. Fitting and "prediction" of the temperature dependences of the rate constants of reactions 8 (Cl + CH_4), 11 (Cl + $CHCl_3$), and 18 (Cl + CH_3Br). Symbols: experimental data, dotted lines: results of fitting using the second approach (only E_0 is adjusted, BH&HLYP/6-311G(d,p) molecular structures and frequencies are used), solid lines: "predicted" temperature dependences (BH&HLYP/6-311+G(3df,2pd)//BH&HLYP/6-311G(d,p)-based analysis; see Discussion). Experimental data are from refs 10 (squares), 57 (open circles), 58 (filled circles), 66 (open triangles), and 67 (filled triangles). This plot provides examples of the best, average, and worst cases of deviation from the best fit line in the $E_{0,CALC}$ vs $E_{0,EXP}$ correlation obtained using the above quantum chemical method (see Discussion). Rate constants of reactions 11 and 18 are multiplied by 0.1 and 10, respectively, to avoid plot congestion.

In the current work, the "experimental" energy barriers were evaluated by fitting of the experimental temperature dependences of the reaction rate constants with transition state theory based models created on the basis of quantum chemical calculations. Two approaches were initially used. In the first approach, the model of a particular reaction is adjusted to provide a match with the experimental data by varying two parameters: the barrier height, E_0, and the preexponential correction factor, F_A. The latter has the meaning of the ratio of the calculated to the experimental preexponential factors. In the second approach, the experimental rate constant temperature dependence is fitted using a quantum chemistry based model with only one adjustable parameter, the energy barrier E_0. Vibrational frequencies of the transition state (responsible for the entropic, or preexponential, factor) obtained from quantum chemical calculations are thus used without any modifications. This second approach is illustrated in Figure 1, where the experimental temperature dependences of the rate constants of reactions 8 (Cl + CH_4), 11 (Cl + $CHCl_3$), and 18 (Cl + CH_3Br) are displayed along with the lines obtained in the fitting.

While the first approach requires reliable knowledge of the temperature dependence of the rate constant over a wide range of temperatures, the second approach can be used even if only the room-temperature value of the rate constant is known. Analysis of the values of the preexponential correction factors, F_A, and those of the reaction energy barriers obtained through the first and the second approaches allows the assessment of the uncertainties resulting from the use of only one adjustable parameter in the second approach (see section III). When the second approach is used, the fitted value of the "experimental" energy barrier acquires the meaning of the barrier value needed to reproduce the experimental data (on average, over the given temperature range) using a particular quantum chemical method

TABLE 1: Experimental Data Set

no.	reaction	A[a]	n[a]	E_a[a]	k(298 K)	T/K	exptl method[b]	refs
8	$Cl + CH_4 \rightarrow HCl + CH_3$	5.69×10^{-19}	2.49	609	1.1×10^{-13}	200−1104	DF/RF, FP/RF	10, 57[c]
9	$Cl + CH_3Cl \rightarrow HCl + CH_2Cl$	2.03×10^{-13}	0.70	915	5.1×10^{-13}	222−843	DF/RF, FP/RF, RR	10, 58, 59[d,e]
10	$Cl + CH_2Cl_2 \rightarrow HCl + CHCl_2$	1.86×10^{-16}	1.55	382	3.5×10^{-13}	222−790	DF/RF, RR	10, 59[d,e]
11	$Cl + CHCl_3 \rightarrow HCl + CCl_3$	2.55×10^{-16}	1.41	641	9.1×10^{-14}	298−854	DF/RF, DF/MS	10, 60[e]
12	$Cl + CH_3F \rightarrow HCl + CH_2F$	4.79×10^{-12}	0.00	772	3.6×10^{-13}	216−296	FP/RF	58
13	$Cl + CH_2F_2 \rightarrow HCl + CHF_2$				3.2×10^{-14}	295	RR	61[f,g]
14	$Cl + CHF_3 \rightarrow HCl + CF_3$	9.53×10^{-13}	0.00	3730	3.5×10^{-18}	303−399	RR	62[f,h]
15	$Cl + CH_2FCl \rightarrow HCl + CHFCl$				1.1×10^{-13}	295, 298	RR	63, 64[f]
16	$Cl + CHF_2Cl \rightarrow HCl + CF_2Cl$	4.00×10^{-12}	0.00	2321	1.7×10^{-15}	296−411	DF/MS	60, 65[i]
17	$Cl + CHFCl_2 \rightarrow HCl + CFCl_2$	5.20×10^{-12}	0.00	1675	1.9×10^{-14}	298−433	DF/MS	60[j]
18	$Cl + CH_3Br \rightarrow HCl + CH_2Br$	5.52×10^{-12}	0.16	1030	4.3×10^{-13}	222−394	FP/RF, VLPR/MS	66, 67[k]
19	$Cl + CH_2Br_2 \rightarrow HCl + CHBr_2$	5.54×10^{-16}	1.40	412	4.0×10^{-13}	222−395	FP/RF, VLPR/MS	66, 67[k]
20	$Cl + CHBr_3 \rightarrow HCl + CBr_3$	4.30×10^{-12}	0.00	809	2.9×10^{-13}	273−363	VLPR/MS	67
21	$Cl + CHF_2Br \rightarrow HCl + CF_2Br$				6.2×10^{-15}	296	RR	56[f]
22	$Cl + CH_2ClBr \rightarrow HCl + CHClBr$				4.7×10^{-13}	296	RR	68, 69[f]
23	$Cl + CHCl_2Br \rightarrow HCl + CCl_2Br$				1.6×10^{-13}	296	RR	69[f]
24	$Cl + CHClBr_2 \rightarrow HCl + CClBr_2$				2.1×10^{-13}	296	RR	69[f]

[a] Parameters of modified Arrhenius dependences ($k = AT^n \exp(-E_a/T)$) in units of cm^3 $molecule^{-1}$ s^{-1} and K. These parameters are given for information only. Individual data points were used in fits. [b] Experimental methods used. DF, discharge flow; RF, resonance fluorescence; FP, flash photolysis; RR, relative rates; MS, mass spectrometry; VLPR, very low pressure reactor. [c] Combined set of data from refs 10 and 57. Results of numerous other direct determinations of the rate constant of reaction 8 are in agreement with this temperature dependence of k_8, as discussed in ref 10. [d] Here, the relative rates data of ref 59 were converted to the values of k_9 and k_{10} using the $k_8(T)$ dependence of equation IX of ref 10. [e] See discussion of experimental data in ref 10. [f] Relative rates data were converted to the absolute values of the rate constant using the $k_8(T)$ dependence of equation X of ref 10. [g] There is a factor of 2 disagreement with the earlier larger value of ref 70. [h] The results of a relative rates study of Coomber and Whittle are preferred over those of Jourdain et al.[71] (larger by more than 2 orders of magnitude) following the recommendation of ref 72. [i] Results of the relative rates study of ref 63 are in agreement with those of refs 65 and 60. [j] Results of the relative rates study of ref 63 are in agreement with those of ref 60. [k] Results of the relative rates study of ref 73 are in agreement with those of refs 66 and 67; rate constant values of ref 74 (relative rates) are ∼25% larger.

for the calculation of the structures and vibrational frequencies of the reactants and the transition state involved. In comparison with the real energy barriers, barrier values obtained through the second approach can be expected to have larger errors because errors due to the imperfect description of the preexponential factor using a particular quantum chemical method are added to the errors due to imperfect reaction rate theory.

II.2.4. Method of Calculation of the Rate Constants. Rate constant values were calculated using the classical transition state theory formula (see, for example, ref 41). Quantum tunneling correction was computed using the "barrier width" method.[11,12,42,43] The shape of the reaction potential energy barrier was determined using the method of reaction path following (intrinsic reaction coordinate, IRC)[44,45] in mass-weighted internal coordinates. The resultant barrier potential energy profiles were fitted with the unsymmetrical Eckart function[46] to determine the "width" parameter l which was used in the calculation of the tunneling correction. Details of the computational approach can be found in refs 12 and 11. Knowledge of the reaction enthalpies is needed for calculation of the tunneling corrections. Experimental values[47−52] of the heats of formation of the reactants and radical products were used for those reactions for which this information is available. For those reaction channels for which the experimental thermochemical data on the radical products R are not available, isodesmic reactions of the types

$$R + CH_4 = RH + CH_3 \qquad (7)$$

were used. A reaction path degeneracy value of 2 (due to optical isomerism in the transition states[53−55]) was used for reactions 15 and 22 (see Table 1 for reaction numbering). For all reactions, the contributions to the reaction path degeneracy resulting from the ratio of the rotational symmetry numbers of the reactants and the transition states were taken into account by including the symmetry numbers directly in the respective rotational partition functions.

II.3. Experimental Data Set. Experimental data on the rate constants of 17 reactions of Cl atom with methane and halogenated methanes are available in the literature. These reactions are presented in Table 1 along with the sources of this information.[10,56−74] For some of the reactions, several sources of rate constant values are available. In such cases, preference is given to data obtained in direct experiments. The rate constant temperature dependences are known over wide ranges of temperatures for only four of these reactions (reactions 8−11). For other reactions, the experimental data cover smaller temperature ranges or exist only at room temperature.

The reactions of Cl atom with methane and chlorinated and fluorinated methanes form a smaller subset of 10 reactions henceforth denoted as the "small set." Calculations based on MP2-level and QCISD-level structures and vibrational frequencies of the species involved were limited to this small set of reactions. Reactions of species containing Br atoms were excluded from this small set because of the excessive computational resources needed for their treatment. Calculations based on the BH&HLYP-level structures and frequencies used both the small set and the complete set of reactions (also referred to as the "large set" henceforth).

III. Results

III.1. "Experimental" Values of Energy Barriers and Preexponential Correction Factors. Table 2 presents the results of fitting of the experimental rate constant data with quantum chemistry based models. The first approach (fitting both E_0 and F_A, see above) was used for those reactions for which temperature dependences obtained in direct experiments are available; the second approach (fitting only E_0) was used for all reactions. The values of the preexponential correction factors in Table 2 vary from 0.48 to 3.02; those obtained in modeling of reactions 8−11, for which temperature dependences over wide temperature intervals are established, range from 0.89 to 2.52. The average values of F_A obtained are 1.24, 1.50, and

TABLE 2: Results of Fitting of the Experimental Rate Constant Data with Quantum Chemistry Based Models

		MP2 model[c]			QCISD model[d]			BH&HLYP model[e]		
		1st appr[f]		2nd appr[g]	1st appr[f]		2nd appr[g]	1st appr[f]		2nd appr[g]
no.[a]	RH[b]	E_0[h]	F_A[i]	E_0[h]	E_0[h]	F_A[i]	E_0[h]	E_0[h]	F_A[i]	E_0[h]
8	CH_4	13.11	1.78	14.82	11.18	2.52	13.59	13.44	1.77	15.19
9	CH_3Cl	8.36	0.89	8.02	7.77	1.09	8.01	8.34	0.90	8.04
10	CH_2Cl_2	4.85	1.31	5.69	4.92	1.43	6.08	5.06	1.30	5.90
11	$CHCl_3$	5.15	1.10	5.50	5.30	1.18	5.94	5.43	1.13	5.89
12	CH_3F	5.10	2.51	6.99	4.94	3.02	7.21	5.10	2.61	6.99
13	CH_2F_2			13.27			13.22			12.94
14	CHF_3			34.26			34.24			34.42
15	CH_2FCl			9.15			9.70			9.60
16	CHF_2Cl	21.08	0.49	18.78	20.38	0.62	18.86	19.13	0.73	18.14
17	$CHFCl_2$	12.53	0.63	10.97	12.84	0.64	11.32	12.68	0.63	11.10
18	CH_3Br							9.23	0.55	7.62
19	CH_2Br_2							5.86	0.75	4.96
20	$CHBr_3$							4.04	0.48	1.67
21	CHF_2Br									14.53
22	CH_2ClBr									4.61
23	$CHCl_2Br$									6.14
24	$CHClBr_2$									5.02

[a] Reaction number (see Table 1). [b] RH substrate in the Cl + RH reaction. [c] Models based on MP2/6-311G(2d,2p)-optimized structures and vibrational frequencies. [d] Models based on QCISD/6-311G(d,p)-optimized structures and vibrational frequencies. [e] Models based on BH&HLYP/6-311G(d,p)-optimized structures and vibrational frequencies. [f] First approach in data fitting, as described in section II.2. Both E_0 and F_A are adjusted in the fits. [g] Second approach in data fitting, as described in section II.2. Only E_0 is adjusted in the fits. [h] Energy barrier in kJ mol^{-1}. [i] Preexponential correction factor (see section II.1).

TABLE 3: Values of the Energy Barriers for Reactions 8−17 (Small Set) Calculated Using Structures Optimized with the MP2 Method[a]

		barrier energies/kJ mol^{-1}							
no.[b]	RH[c]	UMP2[d]	PMP2[e]	PMP2/L[f]	PMP4/L[g]	QCISD/l[h]	QCISD(T)/l[i]	UMP2/DZ[j]	PMP2/DZ[k]
8	CH_4	21.48	13.44	8.61	15.38	22.96	30.21	15.67	7.20
9	CH_3Cl	13.93	4.30	−3.42	3.19	12.80	22.83	8.43	−1.42
10	CH_2Cl_2	9.37	−0.27	−8.89	−3.27	6.70	17.97	5.80	−2.57
11	$CHCl_3$	7.36	−1.01	−10.90	−6.59	3.75	15.25	3.20	−4.05
12	CH_3F	10.20	0.72	0.34	5.86	14.66	23.59	12.05	2.22
13	CH_2F_2	13.75	3.80	4.18	8.39	17.79	27.65	18.56	8.42
14	CHF_3	37.34	27.26	26.20	30.27	40.38	50.94	41.26	30.93
15	CH_2FCl	11.82	1.92	−2.79	2.08	11.90	22.55	11.59	2.09
16	CHF_2Cl	22.31	12.09	7.75	12.06	23.12	34.35	23.16	12.85
17	$CHFCl_2$	13.04	3.51	−3.71	0.64	11.50	22.98	11.16	2.28

[a] Barrier energies with the contributions of the ZPE included. Structures were optimized using the MP2/6-311G(2d,2p) method for all single-point calculations except those denoted as UMP2/DZ and PMP2/DZ, for which the MP2/aug-cc-pvdz optimization method was used. [b] Reaction number (see Table 1). [c] RH substrate in the Cl + RH reaction. [d] UMP2/6-311G(2d,2p). [e] PMP2/6-311G(2d,2p). [f] PMP2/6-311++G(3df,2p). [g] PMP4(SDTQ)/6-311++G(3df,2p). [h] QCISD/6-311+G(2d,2p). [i] QCISD(T)/6-311+G(2d,2p). [j] UMP2/aug-cc-pvdz. [k] PMP2/aug-cc-pvdz.

1.08 for the MP2-, QCISD-, and BH&HLYP-based models, respectively. These values are reasonably close to unity, which justifies the use of calculated transition state properties and the resultant preexponential factors in the fitting performed under the second approach. The scatter of individual F_A values, however, demonstrates that the use of quantum chemistry based preexponential factors can introduce noticeable errors, which propagate into the values of the fitted "experimental" energy barriers. The resultant average uncertainty in the fitted energy barriers can be evaluated from the approximate average factor of 2 uncertainty in the preexponential factor and the fact that most of the experimental data are located around room temperature. This factor of 2 at room temperature translates into a 1.7 kJ mol^{-1} uncertainty in the fitted energy barrier when quantum chemistry based preexponential factors are used.

The treatment of tunneling provides an additional source of uncertainty, which can be estimated from the variations obtained using somewhat different values of the barrier widths resulting from the use of different quantum chemical methods. This average uncertainty due to tunneling is estimated as a factor of 1.5 at room temperature, which translates into an additional uncertainty of 1 kJ mol^{-1} for the fitted energy barriers. The total estimated uncertainty for the "experimental" energy barriers obtained with the second approach (fitting of E_0 using quantum chemistry based preexponential factors) is, thus, 2.7 kJ mol^{-1}. This value is consistent with the differences between the barrier energies obtained for individual reactions using different models (Table 2). It should be noted here that this estimated average uncertainty is meaningful only within the framework of the theoretical methods used, i.e., classical transition state theory[41] with one-dimensional tunneling correction via the "barrier width" method.[11,12,42,43] Issues related to such effects as multidimensional tunneling or variational effects have been intentionally left out of the methodology used in the current study. Actual differences between the "experimental" barriers and the real energies of the saddle points of the potential energy surfaces can be larger.

III.2. Correlations between the Calculated and the "Experimental" Energy Barriers. Tables 3−5 present the values of the energy barriers for reactions 8−17 (Tables 3 and 4, small set) and 8−24 (Table 5, large set) obtained with various single-point quantum chemical methods using geometrical structures optimized in MP2, QCISD, and BH&HLYP calculations. As discussed in section II.1, under the primary assumption of the

TABLE 4: Values of the Energy Barriers for Reactions 8−17 (Small Set) Calculated Using Structures Optimized with the QCISD Method[a]

		barrier energies/kJ mol^{-1}			
no.[b]	RH[c]	QCISD[d]	PMP2/L[e]	QCISD/l[f]	QCISD(T)/l[g]
8	CH_4	36.00	5.10	22.92	30.03
9	CH_3Cl	27.82	−6.46	12.41	22.65
10	CH_2Cl_2	23.32	−13.35	6.09	17.91
11	$CHCl_3$	21.52	−17.56	3.17	15.94
12	CH_3F	25.37	−3.38	14.25	23.21
13	CH_2F_2	29.14	−0.13	17.45	27.60
14	CHF_3	52.65	22.47	39.60	50.19
15	CH_2FCl	26.27	−6.98	11.56	22.63
16	CHF_2Cl	37.59	3.82	22.56	34.10
17	$CHFCl_2$	27.79	−8.92	11.12	23.40

[a] Barrier energies with the contributions of the ZPE included. Structures were optimized using the QCISD/6-311G(d,p) method. [b] Reaction number (see Table 1). [c] RH substrate in the Cl + RH reaction. [d] QCISD/6-311G(d,p). [e] PMP2/6-311++G(3df,2pd). [f] QCISD/6-311+G(2d,2p). [g] QCISD(T)/6-311+G(2d,2p).

technique of isodesmic reactions for transition states, plots of the calculated vs "experimental" energy barriers for a series of reactions of the same type should form straight lines with slopes equal to unity. Examples of such dependences are presented in Figures 2−4. Energy barriers calculated using structures optimized with a particular quantum chemical method (e.g., MP2) are compared to the "experimental" values derived from the experimental data using the transition state theory models based on the molecular structures and frequencies obtained in calculations using the same quantum chemical method. As can be seen from the plots, the expected linear correlations are, indeed, observed. The degrees of correlation, or the "quality" of these linear plots, differ from one quantum chemical method to another. In the current study, 21 combinations of single-point energy methods with those of geometry optimization have been used; presenting all the calculated vs "experimental" barrier plots in the article is impractical. Instead, Figures 2−4 display the "best" and the "worst" plots for each of the quantum chemical methods used for optimization of structures. A complete set of plots is given in the Supporting Information. Tables 6 and 7 present the parameters of the fitted lines (intercepts) and the average and the maximum absolute deviations from the lines for all quantum chemical methods used.

IV. Discussion

Observation of the expected linear correlation between the calculated and the "experimental" values of the energy barriers (Figures 2−4) provides support for the basic underlying postulate of the technique of isodesmic reactions for transition states (see section II.2). The amount of scatter of the individual points around the best fit lines depends on the quantum chemical methods used. It should be noted that ideal linear correlations are not expected because of the finite accuracy of the determination of the "experimental" energy barriers. As described in section III.1, the average uncertainty of these "experimental" energy barriers is estimated as 2.7 kJ mol^{-1}. Thus, the degree of scatter beyond the ±2.7 kJ mol^{-1} envelopes around the best fit lines in the plots of the calculated vs the "experimental" values of E_0 indicates the accuracy of a particular quantum chemical method achieved within the technique of isodesmic reactions for transition states. A convenient quantitative measure of this accuracy is the maximum absolute deviation from the best fit line beyond the expected ±2.7 kJ mol^{-1} envelope of scatter (Tables 6 and 7).

For each quantum chemical method used, the intercept of the best fit line with the *Y*-axis (Tables 6 and 7) provides a value of the systematic deviation of the calculated barrier from the value needed to accurately describe the rate constants. Not surprisingly, computationally expensive higher level methods such as PMP4/6-311++G(3df,2p), QCISD(T)/6-311+G(2d,2p), and CCSD(T)/6-311+G(2d,2p) show the smallest systematic deviations.

Examination of the maximum deviations beyond the expected ±2.7 kJ mol^{-1} envelope of scatter (Tables 6 and 7) provides the following observations. Higher level methods (PMP4, QCISD(T), and CCSD(T) with large basis sets) yield larger scatter: 2.9−4.1 kJ mol^{-1}. The PMP2 method with large basis sets performed the worst: 2.7−6.5 kJ mol^{-1}. At the same time, lower level methods yielded better results. Surprisingly, the

TABLE 5: Values of the Energy Barriers for Reactions 8−24 (Large Set) Calculated Using Structures Optimized with the BH&HLYP Method[a]

		barrier energies/kJ mol^{-1}								
no.[b]	RH[c]	BH&HLYP[d]	BH&HLYP/L[e]	KMLYP/L[f]	PMP2/L[g]	QCISD/l[h]	QCISD(T)/l[i]	CCSD/l[j]	CCSD(T)/l[k]	BH&HLYP/TZ[l]
8	CH_4	22.89	18.55	−0.97	5.08	29.53	22.63	29.84	22.88	21.59
9	CH_3Cl	19.03	11.45	−11.48	−7.64	21.77	11.76	22.93	12.44	15.61
10	CH_2Cl_2	17.49	8.45	−15.81	−15.28	17.50	5.53	18.93	6.38	13.63
11	$CHCl_3$	17.85	8.24	−16.41	−19.68	15.61	2.60	17.13	3.52	14.49
12	CH_3F	11.79	10.54	−11.80	−3.78	23.06	14.21	24.26	14.80	13.79
13	CH_2F_2	16.55	14.00	−9.41	−0.75	27.41	17.37	28.85	18.09	18.08
14	CHF_3	43.80	38.40	16.58	22.40	50.01	39.68	51.41	40.40	43.22
15	CH_2FCl	17.62	11.21	−12.62	−8.43	22.07	11.00	23.56	11.81	15.83
16	CHF_2Cl	30.86	23.57	0.52	2.86	33.61	22.16	35.13	22.98	28.79
17	$CHFCl_2$	22.77	14.20	−9.82	−10.56	22.94	10.57	24.50	11.46	19.99
18	CH_3Br	20.22	14.98	−7.79		22.56	12.74	24.03	13.55	
19	CH_2Br_2	16.51	10.99	−12.84		16.71	4.92	18.56	5.95	
20	$CHBr_3$	14.09	8.34	−15.61		11.57	−1.33	13.59	−0.18	
21	CHF_2Br	25.90	20.32	−2.36		28.84	17.29	30.50	18.19	
22	CH_2ClBr	16.95	9.67	−14.36		16.98	5.11	18.62	6.05	
23	$CHCl_2Br$	16.32	8.10	−16.29		14.05	1.07	15.73	2.06	
24	$CHClBr_2$	15.09	8.09	−16.06		12.64	−0.32	14.48	0.75	

[a] Barrier energies with the contributions of the ZPE included. Structures were optimized using the BH&HLYP/6-311G(d,p) method for all single-point calculations except those denoted as BH&HLYP/TZ, for which the BH&HLYP/aug-cc-pvtz optimization method was used. [b] Reaction number (see Table 1). [c] RH substrate in the Cl + RH reaction. [d] BH&HLYP/6-311G(d,p). [e] BH&HLYP/6-311+G(3df,2p). [f] KMLYP/6-311+G(3df,2p). [g] PMP2/6-311++G(3df,2pd). [h] QCISD/6-311+G(2d,2p). [i] QCISD(T)/6-311+G(2d,2p). [j] CCSD/6-311+G(2d,2p). [k] CCSD(T)/6-311+G(2d,2p). [l] BH&HLYP/aug-cc-pvtz.

TABLE 6: Deviations from the Best Fit Lines on the Plots of the Calculated vs "Experimental" Values of the Energy Barriers and *Y*-Axis Intercepts: Small Reaction Set

method[a]	intercept[b]	av dev[c]	max dev[d]	max dev − 2.7 kJ mol^{-1} [e]
	MP2/6-311G(2d,2p)-Based Models			
UMP2/6-311G(2d,2p)[f]	3.32	1.31	3.35	0.65
PMP2/6-311G(2d,2p)[f]	−6.17	1.49	4.79	2.09
PMP2/6-311++G(3df,2p)[f]	−11.01	2.80	5.39	2.69
PMP4(SDTQ)/6-311++G(3df,2p)[f]	−5.94	3.09	6.51	3.81
QCISD/6-311+G(2d,2p)[f]	14.09	1.78	4.33	1.63
QCISD(T)/6-311+G(2d,2p)[f]	3.81	2.54	5.56	2.86
UMP2/aug-cc-pvdz[g]	2.34	2.49	4.66	1.96
PMP2/aug-cc-pvdz[g]	−6.95	1.78	3.61	0.91
	QCISD/6-311G(d,p)-Based Models			
QCISD/6-311G(d,p)[h]	17.93	1.57	4.47	1.77
PMP2/6-311++G(3df,2pd)[h]	−15.36	3.68	8.14	5.44
QCISD/6-311+G(2d,2p)[h]	13.95	1.79	3.95	1.25
QCISD(T)/6-311+G(2d,2p)[h]	3.30	2.86	6.07	3.37
	BH&HLYP/6-311G(d,p)-Based Models			
BH&HLYP/6-311G(d,p)[i]	9.25	2.57	5.63	2.93
BH&HLYP/6-311+G(3df,2p)[i]	3.04	0.92	2.38	−0.32
KMLYP/6-311+G(3df,2p)[i]	−19.94	1.96	3.78	1.08
PMP2/6-311++G(3df,2pd)[i]	−16.40	4.17	9.17	6.47
QCISD/6-311+G(2d,2p)[i]	13.53	1.70	3.81	1.11
QCISD(T)/6-311+G(2d,2p)[i]	2.93	2.90	6.22	3.52
CCSD/6-311+G(2d,2p)[i]	14.83	1.58	3.60	0.90
CCSD(T)/6-311+G(2d,2p)[i]	3.66	2.79	6.02	3.32
BH&HLYP/aug-cc-pvtz[j]	7.68	1.25	2.96	0.26

[a] Quantum chemical method used for single-point energy calculations. [b] *Y*-axis intercepts (in kJ mol^{-1}) of the lines fitted through the plots of calculated vs "experimental" values of the energy barriers. Also denoted as E_{CORR} in the Discussion section. [c] Average absolute deviations of points from the fitted lines. [d] Maximum absolute deviations of points from the fitted lines. [e] Maximum absolute deviations of points from the fitted lines beyond the estimated ±2.7 kJ mol^{-1} envelope of uncertainty of the "experimental" energy barrier values surrounding the fitted lines. [f] With UMP2/6-311G(2d,2p)-optimized structures. [g] With UMP2/aug-cc-pvdz-optimized structures. [h] With QCISD/6-311G(d,p)-optimized structures. [i] With BH&HLYP/6-311G(d,p)-optimized structures. [j] With BH&HLYP/aug-cc-pvtz-optimized structures.

TABLE 7: Deviations from the Best Fit Lines on the Plots of the Calculated vs "Experimental" Values of the Energy Barriers and *Y*-Axis Intercepts: Large Reaction Set

	BH&HLYP/6-311G(d,p)-based models			
method[a]	intercept[b]	av dev[c]	max dev[d]	max dev − 2.7 kJ mol^{-1} [e]
BH&HLYP/6-311G(d,p)	10.18	2.05	6.56	3.86
BH&HLYP/6-311+G(3df,2p)	3.90	1.53	3.46	0.76
KMLYP/6-311+G(3df,2p)	−19.37	2.07	3.95	1.25
QCISD/6-311+G(2d,2p)	12.60	2.14	4.97	2.27
QCISD(T)/6-311+G(2d,2p)	1.43	3.36	6.76	4.06
CCSD/6-311+G(2d,2p)	14.08	1.94	4.61	1.91
CCSD(T)/6-311+G(2d,2p)	2.26	3.22	6.52	3.82

[a] Quantum chemical method used for single-point energy calculations. BH&HLYP/6-311G(d,p)-optimized structures were used. [b] *Y*-axis intercepts (in kJ mol^{-1}) of the lines fitted through the plots of calculated vs "experimental" values of the energy barriers. Also denoted as E_{CORR} in the Discussion section. [c] Average absolute deviations of points from the fitted lines. [d] Maximum absolute deviations of points from the fitted lines. [e] Maximum absolute deviations of points from the fitted lines beyond the estimated ±2.7 kJ mol^{-1} envelope of uncertainty of the "experimental" energy barrier values surrounding the fitted lines.

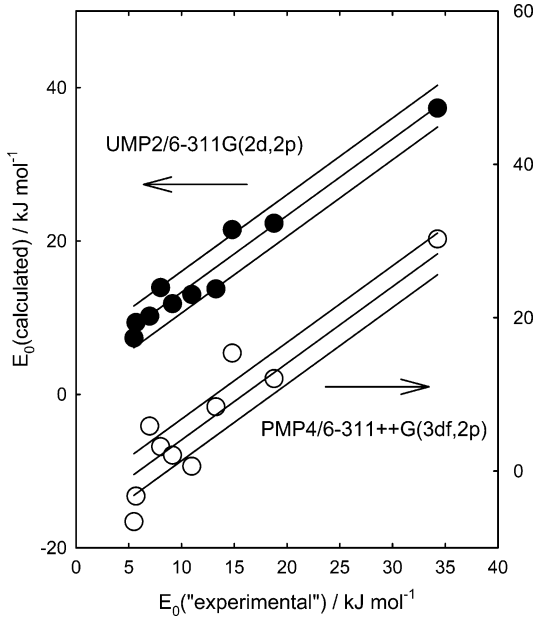

Figure 2. Examples of correlations between calculated and "experimental" values of reaction energy barriers obtained with MP2-based molecular structures and reaction models (small reaction set). A variety of single-point methods for energy calculation was used (Tables 3 and 6); these two plots display only the "best" and the "worst" cases, i.e., the cases of the least and the most scatter around the best fit lines. For each quantum chemical method, three solid lines represent the best fit (middle line) and the ±2.7 kJ mol^{-1} expected envelope of scatter due to the uncertainty in the "experimental" barrier values (upper and lower lines). Note the different *Y*-axes used for the two plots, as indicated by arrows.

QCISD and the CCSD methods (without the triples correction) produced less scatter than the QCISD(T) and the CCSD(T) methods: 0.9−1.25 kJ mol^{-1} for the small set of reactions and up to 2.3 for the large set of reactions. For the MP2-based reaction models, the method used for geometry optimization (UMP2/6-311G(2d,2p)) produced the smallest degree of scatter: only 0.7 kJ mol^{-1} beyond the ±2.7 kJ mol^{-1} envelope (Figure 2); the use of the spin-projected PMP2 method for energy calculation resulted in larger scatter: 2.1 kJ mol^{-1}. Use of the augmented correlation-consistent aug-cc-pvdz basis set in geometry optimization and energy calculations did not improve the amount of scatter. For the QCISD-based reaction models, the use in the energy calculations of the same method

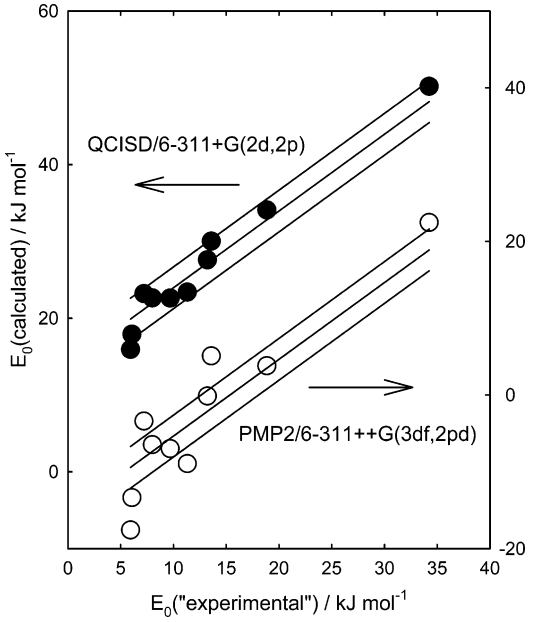

Figure 3. Examples of the correlations between the calculated and the "experimental" values of the reaction energy barriers obtained with QCISD-based molecular structures and reaction models (small reaction set). A variety of single-point methods for energy calculation was used (Tables 4 and 6); these two plots display only the "best" and the "worst" cases, i.e., the cases of the least and the most scatter around the best fit lines. For each quantum chemical method, three solid lines represent the best fit (middle line) and the ± 2.7 kJ mol^{-1} expected envelope of scatter due to the uncertainty in the "experimental" barrier values (upper and lower lines). Note the different *Y*-axes used for the two plots, as indicated by arrows.

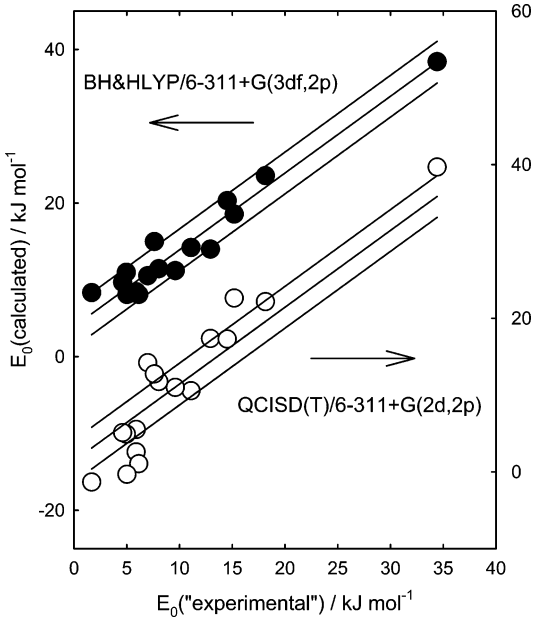

Figure 4. Examples of correlations between calculated and "experimental" values of reaction energy barriers obtained with BH&HLYP-based molecular structures and reaction models (large reaction set). A variety of single-point methods for energy calculation was used (Tables 5 and 7); these two plots display only the "best" and the "worst" cases, i.e., the cases of the least and the most scatter around the best fit lines. For each quantum chemical method, three solid lines represent the best fit (middle line) and the ± 2.7 kJ mol^{-1} expected envelope of scatter due to the uncertainty in the "experimental" barrier values (upper and lower lines). Note the different *Y*-axes used for the two plots, as indicated by arrows.

(QCISD) that was used for geometry optimization also yielded the best results: deviations of 1.8 and 1.3 kJ mol^{-1} beyond the ± 2.7 kJ mol^{-1} envelope with the 6-311G(d,p) and the 6-311+-(2d,2p) basis sets (Figure 3).

For the BH&HLYP-based models, calculations with the small basis set used for geometry optimization (6-311G(d,p)) proved to be insufficient to achieve high accuracy (low scatter) in the barrier energies. However, the use of BH&HLYP energies with a large basis set (6-311+G(3df,2p)) produced excellent results: maximum deviation of less than zero (-0.3 kJ mol^{-1}) with the small set of reactions and 0.8 kJ mol^{-1} beyond the ± 2.7 kJ mol^{-1} envelope with the large set of reactions (Figure 4). Use of a different functional (KMLYP[38,39] with a large basis set) in energy calculations also produced small deviations: 1.1 and 1.3 kJ mol^{-1} beyond the ± 2.7 kJ mol^{-1} envelope for the small and the large sets of reactions, respectively. Calculations performed for the small reaction set with the BH&HLYP/aug-cc-pvtz method used for both geometry optimization and energy calculation also resulted in small deviations: 0.3 kJ mol^{-1}.

It is interesting to note that the BH&HLYP/6-311+G-(3df,2p)//BH&HLYP/6-311G(d.p) method also resulted in small *Y*-axis intercepts (3.0 and 3.9 kJ mol^{-1} for the small and the large reaction sets), indicating small systematic deviation between the calculated and the "experimental" energy barriers. These systematic deviations are similar to those obtained in high-level QCISD(T) and CCSD(T) calculations.

The technique of isodesmic reactions for transition states has been shown[2] to predict energy barriers and rate constants of a series of reactions of H atoms with ethane, chloromethanes, and chloroethanes with a high degree of accuracy. The results of the current study provide further support for this technique, which, in essence, provides a calibration of theory against experiment. Nonzero *Y*-axis intercepts in the plots of the calculated vs the "experimental" energy barriers demonstrate the existence of systematic errors specific to a particular quantum chemical method. The IRTS technique attempts to eliminate these systematic errors. A number of relatively inexpensive quantum chemical methods yield good results, with deviations between the calculated and the "experimental" energy barrier values comparable to the uncertainties of the latter. This accuracy in the energy barrier can be expected to translate into accuracy in the prediction of the rate constants.

The observed linear correlations between the calculated ($E_{0,\mathrm{CALC}}$) and the "experimental" ($E_{0,\mathrm{EXP}}$) energy barriers can be expressed via the equation

$$E_{0,\mathrm{CALC}} = E_{0,\mathrm{EXP}} + E_{\mathrm{CORR}} \qquad \text{(II)}$$

where E_{CORR} is the *Y*-axis intercept. The values of E_{CORR} (Tables 6 and 7) can be used for predictive purposes, as corrections to the calculated barrier values:

$$E_0 = E_{0,\mathrm{CALC}} - E_{\mathrm{CORR}} \qquad \text{(III)}$$

Figure 1 presents examples of such predictive use of eq III for three reactions. Among reactions for which experimental rate constant temperature dependences are available, reactions 8, 11, and 18 represent the best, average, and worst cases of deviation from the best fit line in the $E_{0,\mathrm{CALC}}$ vs $E_{0,\mathrm{EXP}}$ correlation obtained using the BH&HLYP/6-311+G(3df,2pd)//BH&HLYP/6-311G(d,p) method, respectively. As can be seen from the plot, the experimental $k(T)$ dependences are reproduced very well in the cases of the best and average deviations (reactions 8 and 11). In the case of reaction 18 (the worst case), deviation of the calculated rate constant from the experiment reaches a factor of 3.5 at room temperature. Although this deviation may seem

large, it corresponds to a 3 kJ mol^{-1} error in the energy barrier, which is a rather small error for a quantum chemistry derived value.

The calculations performed in the examples illustrated in Figure 1 are not strictly predictive because the values of E_{CORR} (*Y*-axis intercepts) used were derived from the calculated barriers vs "experimental" barriers plot (Figure 4) that included data on the same reactions (8, 11, and 18). However, for each of the reactions considered, removing one data point corresponding to this particular reaction from the correlation plot consisting of 17 points would not change the value of the *Y*-axis intercept in any significant way. Therefore, the examples still serve their purpose: to demonstrate the expected degrees of deviation between the calculated and the experimental values of the rate constants.

The results of the current study indicate the high accuracy of the technique of isodesmic reactions for transition states in its application to the reactions of the Cl + halomethanes class. It is instructive to compare the results with those obtained with high-level quantum chemical methods (such as PMP4 and QCISD(T) with large basis sets) in a more conventional approach, when quantum chemically generated barriers and properties of transition states are used directly to compute reaction rate constants. The lower accuracy of the latter are seen in the systematic errors (as manifested by the *Y*-axis intercepts, E_{CORR}) and the larger scatter of the $E_{0,CALC}$ vs $E_{0,EXP}$ plots. On the other hand, within the technique of isodesmic reactions, even relatively computationally inexpensive quantum chemical methods perform very well; in fact, better than high-level methods used with or without the isodesmic reactions approach.

Acknowledgment. The part of this research performed at The Catholic University of America was supported by the National Science Foundation, Combustion and Thermal Plasmas Program under Grant CTS-9807136. The author thanks Dr. C. A. Gonzalez for helpful advice.

Supporting Information Available: Detailed results of the quantum chemical and rate constants calculations: optimized geometrical configurations (Table 1S); energy values obtained using different computational methods (Table 2S); vibrational frequencies, moments of inertia, and barrier widths associated with individual transition states (Table 3S); 0 K reaction enthalpies of individual reaction channels (Table 4S); and plots of calculated barriers vs "experimental" barrier correlations (Figures 1S−6S). This material is available free of charge via the Internet at http://pubs.acs.org.

References and Notes

(1) Sumathi, R.; Green, W. H. *Theor. Chem. Acc.* **2002**, *108*, 187.
(2) Knyazev, V. D. *J. Phys. Chem. A* **2002**, *106*, 11603.
(3) Karra, S. B.; Gutman, D.; Senkan, S. M. *Combust. Sci. Technol.* **1988**, *60*, 45.
(4) Chang, W. D.; Senkan, S. M. *Environ. Sci. Technol.* **1989**, *23*, 442.
(5) Lee, K. Y.; Yang, M. H.; Puri, I. K. *Combust. Flame* **1993**, *92*, 419.
(6) Taylor, P. H.; Tirey, D. A.; Rubey, W. A.; Dellinger, B. *Combust. Sci. Technol.* **1994**, *101*, 75.
(7) Wang, H.; Hahn, T. O.; Sung, C. J.; Law, C. K. *Combust. Flame* **1996**, *105*, 291.
(8) Ho, W. P.; Yu, Q.-R.; Bozzelli, J. W. *Combust. Sci. Technol.* **1992**, *85*, 23.
(9) Bryukov, M. G.; Slagle, I. R.; Knyazev, V. D. *J. Phys. Chem. A* **2003**, *107*, 6565.
(10) Bryukov, M. G.; Slagle, I. R.; Knyazev, V. D. *J. Phys. Chem. A* **2002**, *106*, 10532.
(11) Bryukov, M. G.; Slagle, I. R.; Knyazev, V. D. *J. Phys. Chem. A* **2001**, *105*, 6900.
(12) Bryukov, M. G.; Slagle, I. R.; Knyazev, V. D. *J. Phys. Chem. A* **2001**, *105*, 3107.
(13) Corchado J. C.; Truhlar D. G.; Espinosa-Garcia, J. *J. Chem. Phys.* **2000**, *112*, 9375.
(14) Michelsen, H. A. *Acc. Chem. Res.* **2001**, *34*, 331.
(15) Roberto-Neto, O.; Coitino, E. L.; Truhlar, D. G. *J. Phys. Chem. A* **1998**, *102*, 4568.
(16) Xiao, J. F.; Li, Z. S.; Ding, Y. H.; Liu, J. Y.; Huang, X. R.; Sun, C. C. *J. Phys. Chem. A* **2002**, *106*, 320.
(17) Xiao, J. F.; Li, Z. S.; Ding, Y. H.; Liu, J. Y.; Huang, X. R.; Sun, C. C. *Phys. Chem. Chem. Phys.* **2001**, *3*, 3955.
(18) Moller, C.; Plesset, M. S. *Phys. Rev.* **1934**, *46*, 618.
(19) Frisch, M. J.; Head-Gordon, M.; Pople, J. A. *Chem. Phys. Lett.* **1990**, *166*, 275.
(20) Head-Gordon, M.; Pople, J. A.; Frisch, M. J. *Chem. Phys. Lett.* **1988**, *153*, 503.
(21) Pople, J. A.; Head-Gordon, M.; Raghavachari, K. *J. Chem. Phys.* **1987**, *87*, 5968.
(22) Becke, A. D. *J. Chem. Phys.* **1993**, *98*, 1372.
(23) Lee, C. T.; Yang, W. T.; Parr, R. G. *Phys. Rev. B* **1988**, *37*, 785.
(24) Frisch, M. J.; Trucks, G. W.; Schlegel, H. B.; Scuseria, G. E.; Robb, M. A.; Cheeseman, J. R.; Zakrzewski, V. G.; Montgomery, J. A., Jr.; Stratmann, R. E.; Burant, J. C.; Dapprich, S.; Millam, J. M.; Daniels, A. D.; Kudin, K. N.; Strain, M. C.; Farkas, O.; Tomasi, J.; Barone, V.; Cossi, M.; Cammi, R.; Mennucci, B.; Pomelli, C.; Adamo, C.; Clifford, S.; Ochterski, J.; Petersson, G. A.; Ayala, P. Y.; Cui, Q.; Morokuma, K.; Malick, D. K.; Rabuck, A. D.; Raghavachari, K.; Foresman, J. B.; Cioslowski, J.; Ortiz, J. V.; Baboul, A. G.; Stefanov, B. B.; Liu, G.; Liashenko, A.; Piskorz, P.; Komaromi, I.; Gomperts, R.; Martin, R. L.; Fox, D. J.; Keith, T.; Al-Laham, M. A.; Peng, C. Y.; Nanayakkara, A.; Gonzalez, C.; Challacombe, M.; Gill, P. M. W.; Johnson, B.; Chen, W.; Wong, M. W.; Andres, J. L.; Gonzalez, C.; Head-Gordon, M.; Replogle, E. S.; Pople, J. A. *Gaussian 98*, Revision A.7; Gaussian, Inc.: Pittsburgh, PA, 1998.
(25) Certain commercial instruments and materials are identified in this article to adequately specify the procedures. In no case does such identification imply recommendation or endorsement by NIST, nor does it imply that the instruments or materials are necessarily the best available for this purpose.
(26) Durant, J. L. *Chem. Phys. Lett.* **1996**, *256*, 595.
(27) Duncan, W. T.; Truong, T. N. *J. Chem. Phys.* **1995**, *103*, 9642.
(28) Maity, D. K.; Duncan, W. T.; Truong, T. N. *J. Phys. Chem. A* **1999**, *103*, 2152.
(29) Truong, T. N. *J. Chem. Phys.* **1994**, *100*, 8014.
(30) Truong, T. N.; Duncan, W. T.; Bell, R. L. *Chemical Applications of Density Functional Theory*; American Chemical Society: Washington, DC, 1996; p 85.
(31) Mora-Diez, N.; Boyd, R. J. *J. Phys. Chem. A* **2002**, *106*, 384.
(32) Kendall, R. A.; Dunning, T. H., Jr.; Harrison, R. J. *J. Chem. Phys.* **1992**, *96*, 6796.
(33) Schlegel, H. B. *J. Phys. Chem.* **1988**, *92*, 3075.
(34) Krishnan, R.; Pople, J. A. *Int. J. Quantum Chem.* **1978**, *14*, 91.
(35) Louis, F.; Gonzalez, C. A.; Huie, R. E.; Kurylo, M. J. *J. Phys. Chem. A* **2000**, *104*, 2931.
(36) Louis, F.; Gonzalez, C. A.; Huie, R. E.; Kurylo, M. J. *J. Phys. Chem. A* **2000**, *104*, 8773.
(37) Louis, F.; Gonzalez, C. A.; Huie, R. E.; Kurylo, M. J. *J. Phys. Chem. A* **2001**, *105*, 1599.
(38) Senosiain, J. P.; Han., J. H.; Musgrave, C. B.; Golden, D. M. *Faraday Discuss.* **2001**, *119*, 173.
(39) Kang, J. K.; Musgrave, C. B. *J. Chem. Phys.* **2001**, *115*, 11040.
(40) Foresman, J. B.; Frisch, A. E. *Exploring Chemistry With Electronic Structure Methods*, 2nd ed.; Gaussian, Inc.: Pittsburgh, PA, 1996.
(41) Johnston, H. S. *Gas-Phase Reaction Rate Theory*; The Ronald Press: New York, 1966.
(42) Knyazev, V. D.; Bencsura, A.; Stoliarov, S. I.; Slagle, I. R. *J. Phys. Chem.* **1996**, *100*, 11346.
(43) Knyazev, V. D.; Slagle, I. R. *J. Phys. Chem.* **1996**, *100*, 16899.
(44) Fukui, K. *Acc. Chem. Res.* **1981**, *14*, 363.
(45) Gonzalez, C.; Schlegel, H. B. *J. Phys. Chem.* **1990**, *94*, 5523.
(46) Eckart, C. *Phys. Rev.* **1930**, *35*, 1303.
(47) Chase, M. W., Jr. *J. Phys. Chem. Ref. Data* **1998**, Monograph 9, 1.
(48) *Thermodynamic Properties of Individual Substances*; Gurvich, L. V., Veyts, I. V., Alcock, C. B., Ed., Eds.; Hemisphere: New York, 1992; Vol. 2.
(49) Kerr, J. A. *CRC Handbook of Chemistry and Physics*; Lide, D. R., Ed.; CRC Press: Boca Raton, FL, 1994−1995.
(50) Seetula, J. A.; Russell, J. J.; Gutman, D. *J. Am. Chem. Soc.* **1990**, *112*, 1347.
(51) Hudgens, J. W.; Johnson, R. D. I.; Timonen, R. S.; Seetula, J. A.; Gutman, D. *J. Phys. Chem.* **1991**, *95*, 4400.
(52) Seetula, J. A. *J. Chem. Soc., Faraday Trans.* **1996**, *92*, 3069.

(53) Pechukas, P. *Dynamics of Molecular Collisions*; Miller, W. H., Ed.; Plenum Press: New York, 1976; Part B.
(54) Gilbert, R. G.; Smith, S. C. *Theory of Unimolecular and Recombination Reactions*; Blackwell: Oxford, 1990.
(55) Karas, A. J.; Gilbert, R. G.; Collins, M. A. *Chem. Phys. Lett.* **1992**, *193*, 181.
(56) Bilde, M.; Sehested, J.; Mogelberg, T. E.; Wallington, T. J.; Nielsen, O. J. *J. Phys. Chem.* **1996**, *100*, 7050.
(57) Whytock, D. A.; Lee, J. H.; Michael, J. V.; Payne, W. A.; Stief, L. J. *J. Chem. Phys.* **1977**, *66*, 2690.
(58) Manning, R. G.; Kurylo, M. J. *J. Phys. Chem.* **1977**, *81*, 291.
(59) Orlando, J. J. *Int. J. Chem. Kinet.* **1999**, *31*, 515.
(60) Talhaoui, A.; Louis, F.; Meriaux, B.; Devolder, P.; Sawerysyn, J.-P. *J. Phys. Chem.* **1996**, *100*, 2107.
(61) Nielsen, O. J.; Ellermann, T.; Bartkiewicz, E.; Wallington, T. J.; Hurley, M. D. *Chem. Phys. Lett.* **1992**, *192*, 82.
(62) Coomber, J. W.; Whittle, E. *Trans. Faraday Soc.* **1966**, *62*, 2183.
(63) Tuazon, E. C.; Atkinson, R.; Corchnoy, S. B. *Int. J. Chem. Kinet.* **1992**, *24*, 639.
(64) Wallington, T. J.; Hurley, M. D.; Schneider, W. F.; Sehested, J.; Nielsen, O. J. *Chem. Phys. Lett.* **1994**, *218*, 34.
(65) Sawerysyn, J. P.; Talhaoui, A.; Meriaux, B.; Devolder, P. *Chem. Phys. Lett.* **1992**, *198*, 197.
(66) Gierczak, T.; Goldfarb, L.; Sueper, D.; Ravishankara, A. R. *Int. J. Chem. Kinet.* **1994**, *26*, 719.
(67) Kambanis, K. G.; Lazarou, Y. G.; Papagiannakopoulos, P. *J. Phys. Chem. A* **1997**, *101*, 8496.
(68) Bilde, M.; Sehested, J.; Nielsen, O. J.; Wallington, T. J. *J. Phys. Chem. A* **1997**, *101*, 5477.
(69) Bilde, M.; Wallington, T. J.; Ferronato, C.; Orlando, J. J.; Tyndall, G. S.; Estupinan, E.; Haberkorn, S. *J. Phys. Chem. A* **1998**, *102*, 1976.
(70) Tschuikow-Roux, E.; Yano, T.; Niedzielski, J. *J. Chem. Phys.* **1985**, *82*, 65.
(71) Jourdain, J. L.; Poulet, G.; Barassin, J.; Le Bras, G.; Combourieu, J. *Pollut. Atmos.* **1977**, *75*, 256.
(72) DeMore, W. B.; Sander, S. P.; Golden, D. M.; Hampson, R. F.; Kurylo, M. J.; Howard, C. J.; Ravishankara, A. R.; Kolb, C. E.; Molina, M. J. *JPL Publ.* **1997**, *97-4*.
(73) Orlando, J. J.; Tyndall, G. S.; Wallington, T. J.; Dill, M. *Int. J. Chem. Kinet.* **1996**, *28*, 433.
(74) Tschuikow-Roux, E.; Faraji, F.; Paddison, S.; Niedzielski, J.; Miyokawa, K. *J. Phys. Chem.* **1988**, *92*, 1488.